IOPscience iopscience.iop.org

Home Search Collections Journals About Contact us My IOPscience

Stress fluctuations in granular force networks

This article has been downloaded from IOPscience. Please scroll down to see the full text article.

J. Stat. Mech. (2011) P04002

(http://iopscience.iop.org/1742-5468/2011/04/P04002)

View the table of contents for this issue, or go to the journal homepage for more

Download details:
IP Address: 132.229.212.105
The article was downloaded on 06/04/2011 at 11:18

Please note that terms and conditions apply.

Journal of Statistical Mechanics: Theory and Experiment
An IOP and SISSA journal

Stress fluctuations in granular force networks

Brian P Tighe[1] **and Thijs J H Vlugt**[2]

[1] Instituut-Lorentz, Universiteit Leiden, Postbus 9506, 2300 RA Leiden, The Netherlands
[2] Delft University of Technology, Process and Energy Laboratory, Leeghwaterstraat 44, 2628 CA Delft, The Netherlands
E-mail: btighe@lorentz.leidenuniv.nl and t.j.h.vlugt@tudelft.nl

Received 18 November 2010
Accepted 8 March 2011
Published 4 April 2011

Online at stacks.iop.org/JSTAT/2011/P04002
doi:10.1088/1742-5468/2011/04/P04002

Abstract. The heterogeneous force networks in static granular media are distinguished from other network structures in that they must satisfy constraints of mechanical equilibrium on every vertex/grain. Here we study the statistics of ensembles of hyperstatic frictionless force networks, which are composed of more forces than can be determined uniquely from force balance. Hyperstatic force networks possess degrees of freedom that rearrange one balanced network into another. We calculate the equation of state and demonstrate that the number of rearrangements governs the macroscopic statistical properties of the ensemble, in particular the macroscopic fluctuations of stress, which scale with distance to the isostatic point. We then show that a maximum entropy postulate allows one to quantitatively capture many features of the microscopic statistics. All predictions are tested against highly accurate Monte Carlo numerical simulations employing umbrella sampling.

Keywords: granular matter, heterogeneous materials (theory), random graphs, networks

J. Stat. Mech. (2011) P04002

©2011 IOP Publishing Ltd and SISSA

Contents

Granular systems are athermal and dissipative: an undriven system will eventually reach a static, mechanically stable state and remain there. By repeatedly applying the same preparation protocol, whether numerically or experimentally, it is possible to build up an ensemble of static granular packings in which each element of the ensemble is a final state of the preparation protocol. Such an ensemble is very different from an equilibrium ensemble: not only is there no thermal equilibrium, there are in fact no dynamics at all.

Micromechanical models like soft spheres interacting via repulsive contact forces provide an attractive way to study granular materials numerically; see, e.g., [1] and references therein. Even at this level of abstraction, however, a theoretical description of the statistical or mechanical properties of disordered packings is daunting. In recent years, a model system called the force network ensemble (FNE) [2] has proven to be an extremely useful tool for studying the disordered stress states of static granular packings. In its simplicity the FNE affords theoretical traction and permits highly accurate simulation, and yet it is detailed enough to reproduce many of the statistical and mechanical properties of numerical and experimental packings [2]–[8]; [9] provides a review.

The force network ensemble is built on the observation that packings of noncohesive frictionless discs or spheres at finite pressure are hyperstatic: they possess a number of contacts in excess of that which would uniquely determine the contact forces from mechanical equilibrium [10]–[12]. This means that for a single packing geometry there exist many different configurations of forces that satisfy force balance on each grain. This indeterminacy can, in principle, be lifted by specifying a contact force law, from which the forces can be determined given the grain positions. The conceit of the FNE, however, is *not* to specify this information, and instead to exploit the force indeterminacy to practical advantage. Because deformations are so small in packings of hard but not perfectly rigid grains, there is a strong separation between the grain scale and the contact scale. The idea is that, by averaging over all balanced force networks on a single frozen contact network,

doi:10.1088/1742-5468/2011/04/P04002

J. Stat. Mech. (2011) P04002

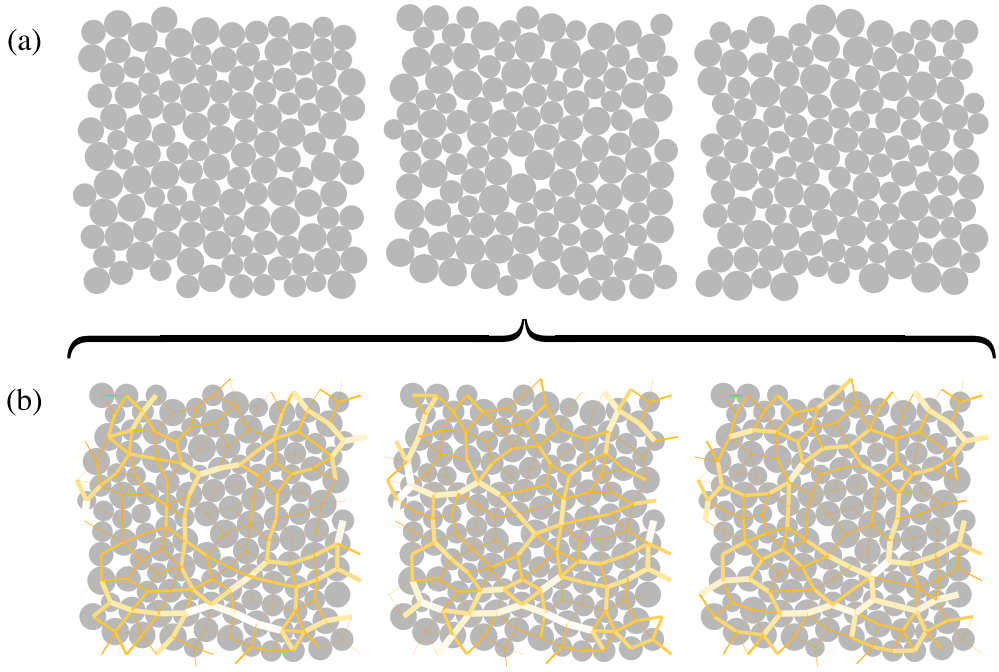

Figure 1. Illustration of two different ensembles. (a) Three periodic packings of 128 particles prepared using molecular dynamics methods. Each packing has the same pressure. (b) Three different force networks, each in balance on the contact network of the central packing of (a). Forces are represented by lines connecting the centers of grains in contact; line thickness is proportional to the force magnitude.

one captures fluctuations in the stresses that would also result from rearrangements of the grain positions. In the FNE, then, *grains* do not rearrange but *forces* do (figure 1).

Here we describe the stress statistics of the force network ensemble within a statistical mechanics framework. The notion of an ensemble description of static granular matter dates to Edwards, who proposed an ensemble of packings characterized by like boundary conditions [13]. Though conceptually appealing, the Edwards ensemble is difficult to probe theoretically. In this spirit the FNE can be seen as a restricted but more accessible version of Edwards' ensemble. In recent years a number of authors have proposed granular ensembles in which stress plays a role similar to that of energy in an equilibrium ensemble [8], [14]–[21], and we shall see that the FNE naturally lends itself to such an approach. The present work represents an elaboration and significant expansion on the results of [8], which demonstrated that the statistics of local stresses within the FNE, in the form of a probability distribution function, can be described *quantitatively* using a maximum entropy principle when local force balance is incorporated in sufficient detail.

This paper is divided in several sections. Section 1 introduces the force network ensemble and motivates its approach to static granular packings. Section 2 develops the FNE in greater detail. We write down the entropy of the canonical FNE and introduce a framework that allows for description of the statistics of macroscopic stresses in the ensemble. We derive for the first time the FNE equation of state. With it we predict, and confirm numerically, the scaling of the macroscopic pressure fluctuations with system size

J. Stat. Mech. (2011) P04002

and average coordination number in the canonical FNE; notably, the relative fluctuations diverge on approach to the critical isostatic coordination number. We then turn to the statistics of local measures of the stress, particularly pressure p at the grain scale; our focus is on the form of the pressure probability distribution function of p for asymptotically small and large p. We demonstrate that the distribution has a Gaussian tail in two dimensions. Finally, section 3 gives a discussion and outlook.

1. Granular ensembles

We are interested in describing the statistics of stresses in static granular packings. To do this, we must first define an ensemble of packings, a task that has drawn considerable interest in recent years [13]–[22]. One obvious choice is the ensemble of all packings having a pressure $\bar{p}$ formed from a collection of N grains. The pressure is a convenient control parameter because it measures the distance to the jamming transition: at $\bar{p} = 0$ the packing loses rigidity [1]. To define this or similar ensembles more precisely, we must first introduce some terminology and express relevant constraints, like mechanical equilibrium, in a convenient form. It will turn out that, in so doing, we lay the groundwork for motivating and constructing the force network ensemble—the model system to be studied in later sections.

In this work we will restrict our attention to frictionless packings of discs. Given the positions of discs in a packing, the contact network is a network of nodes and edges; the nodes are positioned at the centers of grains, while the edges connect nodes of discs that are in contact. For a packing of N grains sharing N_c unique contacts, it is convenient to define the mean coordination number $\bar{z} := 2N_c/N$. We will consider both ordered and disordered contact networks. The disordered networks are generated by a molecular dynamics simulation of soft repulsive discs.

There is a force between every pair of grains in contact, and the forces residing on a contact network constitute a force network. We label a force network with a vector $\mathbf{f} = \{f_{ij}\}$ composed of N_c contact forces between grains. Here $\vec{f}_{ij}$ is the contact force acting on disc i due to disc j; $\vec{f}_{ij} = -\vec{f}_{ji}$ due to Newton's third law, and $\vec{f}_{ij} = \vec{0}$ if i and j are not in contact. For frictionless discs each force must be parallel to the line connecting the centers of the contacting discs, so the force can be represented by a single scalar. Micromechanically this force is determined by the grain positions, but let us for the moment focus on the forces without reference to the force law.

Together the force and contact networks determine the stress tensor $\hat{\bar{\sigma}}$,

$$\hat{\bar{\sigma}} = \frac{1}{2V} \sum_{ij} \vec{f}_{ij} \otimes \vec{r}_{ij}. \tag{1}$$

Here V is the (two-dimensional) volume of the packing, and $\vec{r}_{ij}$ is a vector pointing from the center of disc j to the center of disc i. Note that, by convention, compressive stresses are positive. If the stress is isotropic, we have $\hat{\bar{\sigma}} = \bar{p}\mathbb{1}$, where $\bar{p}$ is the pressure.

For a packing to be static, every disc must be in mechanical equilibrium:

$$\sum_j \vec{f}_{ij} + \vec{F}_i = \vec{0}. \tag{2}$$

J. Stat. Mech. (2011) P04002

Here $\vec{F}_i$ is a body force acting on disc i. We take $\vec{F}_i = \vec{0}$ for every grain; packings will be subjected to a confining stress implemented via periodic boundary conditions. Equation (2) implicitly defines a matrix equation

$$\mathbf{A}\mathbf{f} = \mathbf{0}_{N_c}. \tag{3}$$

$\mathbf{0}_{N_c}$ is the N_c-component vector of zeros. The sparse $2N \times N_c$ matrix $\mathbf{A}$ is determined purely by the geometry of the contact network and is composed of angle cosines described by the edges connecting nodes in the contact network. The matrix $\mathbf{A}$ therefore encodes the constraints of local force balance for a given contact network. Similarly, equation (1), like equation (2), implicitly defines a matrix equation,

$$\mathbf{B}\mathbf{f} = \mathbf{b}, \tag{4}$$

where $\mathbf{b} = (\bar{\sigma}_{xx}, \bar{\sigma}_{yy}, \bar{\sigma}_{xy})$ and $\mathbf{B}$ is a $2N \times 3$ matrix that is determined by the geometry of the contact network.

Let us now define the ensemble of all static packings of N frictionless discs with known radii and a given pressure $\bar{p} = \bar{p}_0$ [1]. The density of states is

$$\Omega(\bar{p}_0) = \int \prod_i \mathrm{d}\vec{r}_i \delta(\mathbf{A}\mathbf{f})\delta(\mathbf{B}\mathbf{f} - \mathbf{b}(\bar{p}_0)), \tag{5}$$

where $\mathbf{A}$, $\mathbf{f}$, $\mathbf{B}$, and $\mathbf{b}(\bar{p}_0)$ are all implicit functions of the positions $\{\vec{r}_i\}$. In recent years, a number of authors have advanced our understanding of such a 'stress ensemble' [14]–[19], [21, 22]. An illustration is given in figure 1(a). Generating such an ensemble in the computer is straightforward, if numerically expensive. While expressions like equation (5) are available, evaluating them analytically is generally difficult or impossible. This opens the door for the force network ensemble, which replaces expressions like equation (5) with a different, physically motivated, more tractable form.

The FNE density of states is

$$\Omega_C^{\mathrm{FNE}}(\bar{p}_0) = \int \prod_{ij} \mathrm{d}f_{ij} \delta(\mathbf{A}\mathbf{f})\delta(\mathbf{B}\mathbf{f} - \mathbf{b}(\bar{p}_0))\Theta(f_{ij}). \tag{6}$$

Let us compare equations (5) and (6). The integral over the $2N$ components of the grain positions in Ω has been replaced by one over N_c contact forces in Ω_C^{FNE}. The subscript indicates that the FNE density of states is defined for a particular, i.e. fixed, contact network C. The function $\Theta(f_{ij})$ is the Heaviside step function; it restricts the integral to force networks in which there are no tensile forces. The same restriction is implicitly present in equation (5) via the force law. Note that $\Omega_C^{\mathrm{FNE}}(\bar{p}_0)$ has a simple geometric interpretation: it is the content of the high-dimensional space of balanced force networks with pressure $\bar{p}_0$. For an isostatic contact network, $\Omega_C^{\mathrm{FNE}}(\bar{p}_0) = 0$; obviously the FNE is trivial in this case. The force network ensemble is therefore appropriate to hyperstatic contact networks, for which a space of force networks can be found and the density of states is nonzero.

The FNE density of states can be motivated by noting that when grains are hard but not perfectly rigid, there is a separation of length scales. Namely, the distance over which a grain must be moved in order to induce a large change in the contact forces is very small compared to the grain scale. The FNE corresponds to the limit in which forces are allowed to fluctuate without *any* change in the grain positions. Thus in the FNE one

J. Stat. Mech. (2011) P04002

replaces an ensemble comprised of many *grain* configurations with an ensemble of many *force* configurations on one fixed contact network (see figure 1(b)). The central conceit of the FNE is that an ensemble of force configurations captures the same fluctuations that would occur if the grain positions were allowed to vary. This is obviously an uncontrolled approximation, but there is now a large body of literature demonstrating the usefulness of the approach. The FNE has been employed fruitfully to describe the statistics of forces in static packings [2, 3, 7, 8], [23]–[25], the volume of the state space in frictionless and frictional packings [26]–[28], bounds on the static yield stress [6], the percolation of force networks through a packing [5, 29], and the response of a packing to boundary forcing [4].

Like many model systems in statistical physics, the FNE is an attempt to provide an understanding of the macroscopic phenomenology of a system without incorporating the microscopic interactions in every detail. Nevertheless, we stress that the FNE includes vector force balance on every grain. Older statistical models such as the q-model [30] employ only an approximate scalar form of force balance. We shall show that the shift from scalar to vector force balance produces not just quantitative but also qualitative changes in the contact force statistics, and therefore vector force balance cannot be neglected.

To further consider the consequences of equation (6), we must introduce the concepts of isostaticity and hyperstaticity [10]–[12]. We will refer to a contact network C as isostatic if there is just one force network satisfying $\mathbf{Af} = \mathbf{0}$ and $\mathbf{Bf} = \mathbf{b}(\bar{p}_0)$.[3] It is therefore convenient to combine equations (3) and (4) in one matrix equation by writing

$$\mathbf{Wf} = \mathbf{c}, \tag{7}$$

where $\mathbf{W} = (\mathbf{A}, \mathbf{B})$ and $\mathbf{c} = (\mathbf{0}_{N_c}, \mathbf{b})$.

A packing's degree of hyperstaticity can be quantified by its mean coordination number, $\bar{z}$. Equation (7) is underdetermined whenever $N_c > 2N + 1$ or, equivalently, $\bar{z} > z_{\mathrm{iso}} = 4 + 1/N$.[4] We will therefore characterize a contact network by its excess coordination $\Delta z := z - z_{\mathrm{iso}}$.

When $\Delta z > 0$, any force network $\mathbf{f}$ satisfying equation (7) can be expressed as [3, 7]

$$\mathbf{f} = \mathbf{f}_0 + \sum_{k=1}^{N_w} c_k \, \delta\mathbf{f}_k. \tag{8}$$

The vector $\mathbf{f}_0$ is a particular solution to equation (4). The $\{\delta\mathbf{f}_k\}$, $k = 1, \ldots, N_w$, are a set of vectors spanning the null space of $\mathbf{W}$. Its nullity, the dimension of its null space, is

$$N_w = \tfrac{1}{2} N \Delta z. \tag{9}$$

Physically, the $\{\delta\mathbf{f}_k\}$ may be understood as states of self-stress of the contact network, while geometrically, N_w is the dimension of the space of force networks. The coefficients $\{c_k\}$ then serve as coordinates of $\mathbf{f}$ in the space of force networks spanned by $\{\delta\mathbf{f}_k\}$, with $\mathbf{f}_0$ as the origin.

[3] Note that the conventional definition of isostatic states imposes force balance but not the stress tensor. We introduce this alteration purely for convenience; it introduces an $O(1/N)$ correction to the isostatic coordination number z_{iso}, which vanishes in the thermodynamic limit.

[4] We have $z_{\mathrm{iso}} = 4 + 2/N$ rather than $4 + 6/N$ because of a peculiarity of periodic boundary conditions. One may show that, even if all contact forces are assigned without regard for local force balance, a periodic packing satisfies $\sum_{ij} \vec{f}_{ij} = 0$. As a consequence only $2N - 2$ of the $2N$ local force balance constraints are independent. When convenient we will gloss over this and other corrections that vanish in the thermodynamic limit.

J. Stat. Mech. (2011) P04002

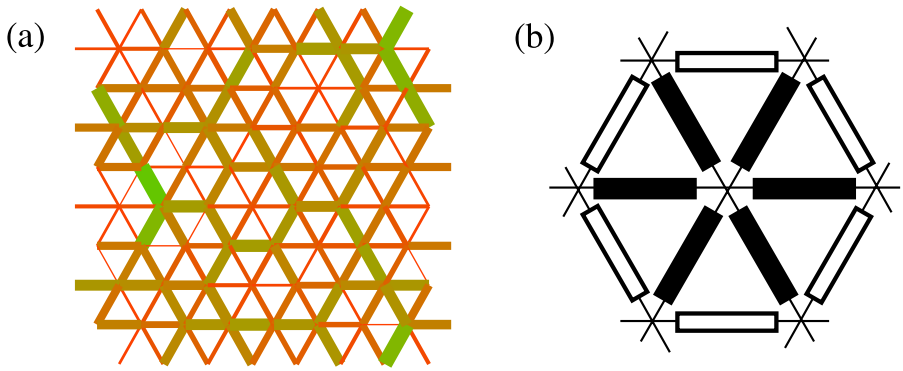

Figure 2. (a) A force network on the frictionless triangular lattice. (b) A Monte Carlo or 'wheel' move in the frictionless triangular lattice [3]. Force is added to spoke contacts (solid bars) and subtracted from six rim contacts (open bars), or vice versa. The net vector force on each of the seven participating grains is unchanged.

Equation (8) is important because it points to a straightforward and efficient way to implement simulations of the FNE. One simply identifies a particular solution $\mathbf{f}_0$ and the null vectors $\{\delta\mathbf{f}_k\}$ by any means convenient. Dynamics in the FNE can then be realized as a random walk in the space of force networks. The null vectors—which we now refer to as force rearrangements—serve as Monte Carlo moves. To sample the space of force networks, Monte Carlo moves are randomly selected and used to update the current force network. The size of the move is uniformly selected from the interval of possible step sizes, determined by the positivity constraint on the affected contact forces[5]. In this way, for sufficiently long runtimes, the space of force networks is sampled with flat measure, i.e. uniformly; see [3] and [7] for details. A particularly simple example of a force rearrangement is the 'wheel move' in the triangular lattice, first introduced in [3] and depicted in figure 2.

We emphasize that, because the force rearrangements are null vectors of $\mathbf{W}$ and because $\mathbf{W}$ imposes the stress tensor of a network, the force rearrangements leave the stress tensor $\hat{\bar{\sigma}}$ invariant. Therefore, trivially, the *extensive* stress $\hat{\mathcal{S}} = \hat{\bar{\sigma}}\mathcal{V}$ is also invariant. The force network ensemble thus bears strong similarity to the microcanonical ensemble. Just as energy is an extensive invariant of the dynamics in an equilibrium system, the extensive stress $\hat{\mathcal{S}}$ is an extensive invariant of the Monte Carlo dynamics of the FNE. Moreover, because 'dynamics' in the FNE are performed by a random walk in the space of force networks, force networks are sampled with equal *a priori* probability. This is again reminiscent of the equilibrium microcanonical ensemble case. In the following, both for simplicity and to reinforce the analogy, we restrict our attention to ensembles of *isotropic* force networks, so that the scalar 'extensive pressure' $\mathcal{P} = \frac{1}{2}\operatorname{Tr}\hat{\mathcal{S}}$ fully specifies the stress, i.e. $\hat{\mathcal{S}} = \mathcal{P}\mathbb{I}$. The extensive pressure is additive, $\mathcal{P} = \sum_{i=1}^{N} p_i$; here

$$p_i = \tfrac{1}{2}\sum_{j=1}^{N} \vec{f}_{ij}\cdot\vec{r}_{ij}, \tag{10}$$

[5] Other sampling methods are possible. For example when employing umbrella sampling (see the appendix), moves are accepted/rejected according to equation (A.3).

J. Stat. Mech. (2011) P04002

and $\vec{f}_{ij}$ is the force on grain i applied by grain j (nonzero only when i and j are in contact) and $\vec{r}_{ij}$ is the vector from the center of j to i. We pursue the analogy to equilibrium ensembles further in the following section.

If the usual definition of the FNE is a microcanonical one, can one pass to a canonical FNE? This question was first considered in detail in [34]; the answer is yes. The isotropic canonical FNE contains one additional force rearrangement that rescales all forces in the network.

2. Statistics in the FNE

In the previous sections we described the force network ensemble and its invariants. We now turn to a study of stress statistics in the ensemble. After writing down and maximizing entropy in the FNE, we consider pressure in the canonical ensemble, deriving the equation of state and the scaling of pressure fluctuations. We then consider the statistics of stress at the grain scale in the form of the local pressure probability distribution $P(p)$.

Because of its similarities to equilibrium ensembles, it is natural to describe the force network ensemble within a statistical mechanics framework. By definition—or alternatively, the Monte Carlo dynamics described above guarantee that—every force network in the FNE is sampled with equal *a priori* probability, i.e. with a flat measure. Here we will write down an entropy, postulate that it is maximized, and show that it correctly reproduces equal *a priori* sampling in the microcanonical FNE. We then follow the same approach to generate a canonical FNE. This approach is in direct analogy to the standard textbook treatment of equilibrium statistical mechanics [35], though we spell out the steps for completeness.

If a force network $\mathbf{f}$ is sampled with frequency $B(\mathbf{f})$, there is an associated entropy

$$S[B] = -\int \mathrm{d}\mathbf{f}\, G(\mathbf{f})[B(\mathbf{f}) \ln B(\mathbf{f})]. \tag{11}$$

The function $G(\mathbf{f})$ restricts the integral to 'valid' states, and is defined to be unity when (i) $\mathbf{f}$ is force balanced, (ii) its contact forces are noncohesive and (iii) the force network is isotropic, i.e. $\bar{\sigma}_{11} = \bar{\sigma}_{22}$ and $\bar{\sigma}_{12} = 0$. $G(\mathbf{f}) = 0$ otherwise. The integral may be further restricted depending on the ensemble under consideration. We postulate that $S[B]$ is maximized subject to certain constraints.

Let us first consider the microcanonical ensemble, in which the relevant constraint is that of normalization:

$$1 = \int_{\mathcal{P}(\mathbf{f})=\mathcal{P}_0} \mathrm{d}\mathbf{f}\, G(\mathbf{f})\, B(\mathbf{f})\,. \tag{12}$$

The integral is restricted to force networks with extensive pressure $\mathcal{P}_0$. The entropy $S[B]$ is maximal for $B(\mathbf{f}) = 1/\Omega(\mathcal{P}_0)$, where

$$\Omega(\mathcal{P}_0) = \int \mathrm{d}\mathbf{f}\, G(\mathbf{f})\, \delta(\mathcal{P}(\mathbf{f}) - \mathcal{P}_0)\,. \tag{13}$$

Note that $B(\mathbf{f})$ is independent of $\mathbf{f}$: all valid force networks in the microcanonical FNE receive the same statistical weight.

J. Stat. Mech. (2011) P04002

An extensive discussion of the microcanonical FNE can be found in [23]. Here we adopt the perspective of a canonical ensemble, in which the extensive pressure $\mathcal{P}(\mathbf{f})$ is allowed to fluctuate; i.e. equation (12) is replaced by

$$1 = \int \mathrm{d}\mathbf{f}\, G(\mathbf{f})\, B(\mathbf{f})\,. \tag{14}$$

At the same time, a constraint on the *average* extensive pressure $\langle\mathcal{P}\rangle$ is imposed:

$$\langle\mathcal{P}\rangle = \int \mathrm{d}\mathbf{f}\, G(\mathbf{f})\, \mathcal{P}(\mathbf{f})\, B(\mathbf{f})\,. \tag{15}$$

We demonstrate below that the microcanonical and canonical ensembles are equivalent in the usual way. Maximizing the entropy subject to the above constraints, one finds that the extremal distribution is

$$B(\mathbf{f}) = Z^{-1} \exp\left(-\alpha \mathcal{P}(\mathbf{f})\right). \tag{16}$$

The Lagrange multiplier α, the inverse of which was termed *angoricity* by Edwards [20], is chosen to satisfy

$$\langle\mathcal{P}\rangle = -\frac{\partial}{\partial\alpha} \ln Z\,, \tag{17}$$

and the partition function Z enforces normalization of $B(\mathbf{f})$:

$$Z(\alpha) = \int \mathrm{d}\mathbf{f}\, G(\mathbf{f})\, \exp\left(-\alpha\mathcal{P}(\mathbf{f})\right). \tag{18}$$

Note that, in perfect analogy to the equilibrium case, force networks in the canonical FNE are weighted by a 'Boltzmann factor' $\exp(-\alpha\mathcal{P})$.

2.1. Macroscopic quantities

It is now straightforward to consider the statistics of the extensive pressure $\mathcal{P}$, including an equation of state relating the intensive parameter α to $\langle\mathcal{P}\rangle$. Our starting point is the partition function Z of equation (18), which may be re-expressed in terms of $\Omega(\mathcal{P})$, the density of states with extensive pressure $\mathcal{P}$:

$$Z = \int_0^\infty \mathrm{d}\mathcal{P}\, \Omega(\mathcal{P})\, \exp\left(-\alpha\mathcal{P}\right). \tag{19}$$

Recall that $\Omega(\mathcal{P})$ is the content of the space of valid force networks with extensive pressure $\mathcal{P}$. The space is a convex polytope in N_w dimensions, and $\mathcal{P}$ sets the typical 'diameter' or linear dimension of the polytope, so $\Omega(\mathcal{P}) \propto \mathcal{P}^{N_\mathrm{w}}$. From equations (13), (17), and (19), it then follows that

$$\alpha\langle\mathcal{P}\rangle = \tfrac{1}{2}\Delta z N + \mathrm{O}(1). \tag{20}$$

Up to corrections that vanish in the thermodynamic limit, equation (20) is the equation of state of the FNE. It simply states that α^{-1} selects the natural pressure scale in the ensemble. This was foreseeable: having discarded the force law, the FNE does not possess an intrinsic force scale, leaving no other scale with which α^{-1} could compete.

J. Stat. Mech. (2011) P04002

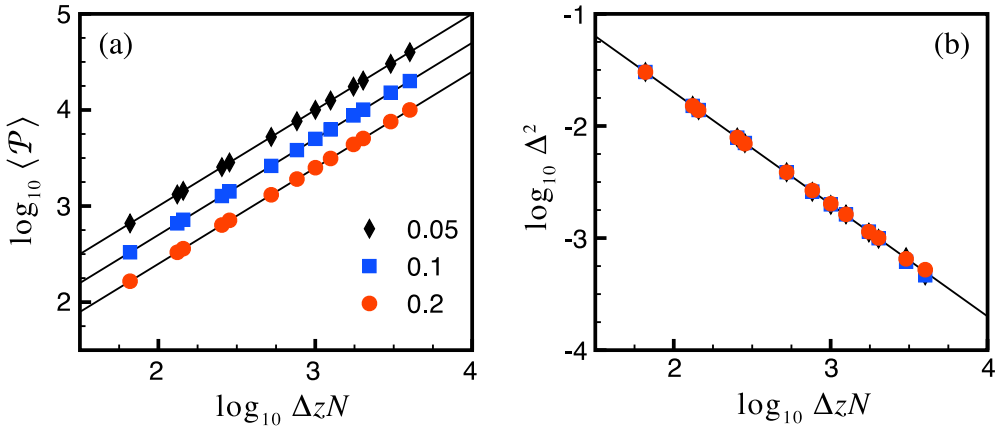

Figure 3. (a) Equation of state for the FNE computed in the canonical ensemble for $\alpha = 0.05$, 0.1, and 0.2, as indicated in the legend. Solid curves are equation (20). For each data point the FNE was simulated on a different contact network. The contact networks were drawn from disordered packings prepared by molecular dynamic simulation of N grains, with N ranging from 250 to 2000; the resulting and mean coordination numbers range from $\bar{z} = 4.25$ to 6.00. Whenever present, rattlers have been removed. (b) The relative fluctuations $\Delta^2 = \langle(\delta\mathcal{P})^2\rangle/\langle\mathcal{P}\rangle^2$ for the same data as in (b) collapse when plotted against $\Delta z\, N$, independently of α, as predicted by equation (22).

The extensive pressure fluctuations can be calculated similarly:

$$\begin{aligned}\langle(\delta\mathcal{P})^2\rangle &= Z^{-1}\int_0^\infty \mathrm{d}\mathcal{P}\,\Omega(\mathcal{P})\,(\mathcal{P}-\langle\mathcal{P}\rangle)^2\exp\left(-\alpha\mathcal{P}\right)\\ &= N_\mathrm{w}/\alpha^2. \end{aligned} \tag{21}$$

Hence the relative fluctuations of pressure are

$$\Delta^2 := \frac{\langle(\delta\mathcal{P})^2\rangle}{\langle\mathcal{P}\rangle^2} = \frac{2}{\Delta z\, N}\,. \tag{22}$$

Note that the pressure fluctuations are governed by N_w, the dimension of the space of valid force networks. The equivalence of canonical and microcanonical ensembles follows from the $1/N$ scaling of the relative fluctuations, which vanish in the thermodynamic limit. Note the dependence on Δz in equation (22), which ensures diverging relative fluctuations in the isostatic limit $\Delta z \downarrow 0$

To test equations (20) and (22), we perform numerical simulations. Frictionless soft sphere packings of varying grain number N and excess coordination Δz are generated with molecular dynamics simulations, and the canonical force network ensemble is sampled on their respective contact networks using Monte Carlo methods. Three different values of the intensive parameter α are used: $\alpha = 0.05$, 0.1, and 0.2. For each contact network we sample the average pressure $\langle\mathcal{P}\rangle$, plotted in figure 3(a), and relative fluctuations Δ^2, plotted in figure 3(b). The data in figure 3(a) are consistent with the equation of state predicted in equation (20). Figure 3(b) plots the pressure fluctuations in simulations of the canonical FNE. The data for a range of N and Δz all fall on the curve described by equation (22). Recall that for each (N, z) pair, three different values of α are plotted; these

J. Stat. Mech. (2011) P04002

are difficult to see because, as predicted by equation (22), the fluctuations are independent of α.

Defining $\rho_{\mathrm{w}} := N_{\mathrm{w}}/\mathcal{V}$, the number density of force rearrangements, the scaling of pressure fluctuations can also be written as $\Delta^2 = 1/\rho_{\mathrm{w}}\mathcal{V}$. Therefore the pressure fluctuations are governed by the ratio of the linear system size $\mathcal{L} := \mathcal{V}^{1/d}$ to the length scale $\ell_{\mathrm{w}} := 1/\rho_{\mathrm{w}}^{1/d} \sim 1/\Delta z^{1/d}$, namely

$$\Delta^2 \sim \left(\frac{\ell_{\mathrm{w}}}{\mathcal{L}}\right)^d. \tag{23}$$

ℓ_{w} sets the scale on which one finds fluctuations on the order of the mean pressure in periodic packings. We stress that ℓ_{w} is different from, though closely related to, the isostatic length $\ell^* \sim 1/\Delta z$ that governs the mechanical response of soft sphere packings [1]. In the FNE the isostatic length describes the typical size of a force rearrangement [28]. The relative pressure fluctuations are not sensitive to the *size* of the force rearrangements, but rather to their *number*, and their number scales as $\mathcal{V}/(\ell_{\mathrm{w}})^d$ rather than $\mathcal{V}/(\ell^*)^d$. This is possible if there is significant spatial overlap between the force rearrangements, i.e. a typical contact participates in multiple rearrangements.

Equivalence of the microcanonical and canonical force network ensemble can be expected only for periodic systems of linear size $\mathcal{L} \gg \ell_{\mathrm{w}}$. In non-periodic systems the balance of boundary and excess bulk contacts again becomes relevant in constructing a canonical ensemble [34]—the system must at a minimum be large enough to support force rearrangements. The isostatic length $\ell^* \gg \ell_{\mathrm{w}}$ as the isostatic limit $\Delta z \downarrow 0$ is approached; hence we anticipate the stricter requirement $\mathcal{L} \gg \ell^*$ for canonical–microcanonical equivalence in non-periodic systems. Nevertheless, the scaling of equation (23) must still hold for asymptotically large non-periodic systems.

2.2. Microscopic quantities

We now turn to the statistics of *local* stresses. One microscopic measure of the stress is the pressure p on an individual grain. Although the distribution of contact forces $P(f)$ is widely studied, we will focus largely on the pressure distribution $P(p)$, which has at least two advantages over $P(f)$. First, p is slightly coarse-grained with respect to f—it is a grain scale rather than contact scale quantity—making it a more realistic target for the approximate expressions that we develop in later sections. Second, it will prove to be convenient that p, being defined on the grain scale, enters at the same scale as the constraints of local force balance.

The local pressure distribution is given by

$$\begin{aligned} P_\mu(p) &= [\Omega(\mathcal{P}_0)]^{-1} \int \mathrm{d}\mathbf{f}\, G(\mathbf{f})\, \delta(\mathcal{P}(\mathbf{f}) - \mathcal{P}_0)\, \delta(p_1(\mathbf{f}) - p) \\ P_\alpha(p) &= [Z(\alpha)]^{-1} \int \mathrm{d}\mathbf{f}\, G(\mathbf{f})\, \mathrm{e}^{-\alpha\mathcal{P}(\mathbf{f})}\, \delta(p_1(\mathbf{f}) - p), \end{aligned} \tag{24}$$

within the microcanonical and canonical FNE indicated by subscripts μ and α, respectively. Here p_1 is the pressure on the grain with index 1 calculated via equation (10). Formally the distribution is particular to the choice of grain on which the pressure p_1 is assigned, unless the contact network is a Bravais lattice, though in practice little difference

J. Stat. Mech. (2011) P04002

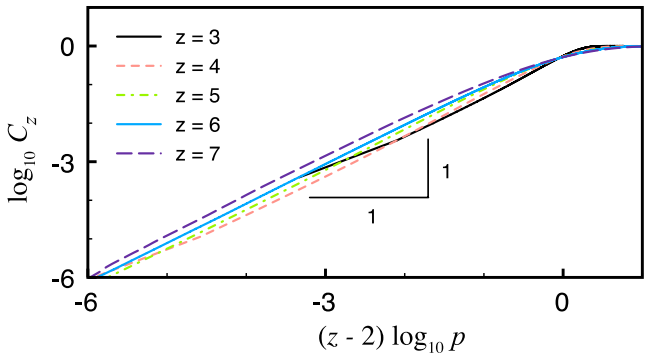

Figure 4. Numerically sampled cumulative distributions $C_z(p) = \int_0^p \mathrm{d}p'\, P(p'|z)$. Statistics are sampled in the microcanonical FNE on a periodic disordered packing in $d = 2$ dimensions generated via molecular dynamics simulation. The packing is composed of 1024 grains sharing 2572 contacts, of which 17 grains have 3 contacts, 233 grains have 4 contacts, 489 grains have 5 contacts, 279 grains have 6 contacts, and 6 grains have 7 contacts.

is found [23]. These two distributions of equations (24) converge to the same form in the thermodynamic limit, as demonstrated numerically in [34]; to study the local stress statistics one may choose to work in whichever ensemble is convenient.

Although equations (24) can be solved exactly for very small systems [3, 23], one must resort to asymptotic or approximate methods in larger systems. We first show that $P(p)$ has a power law form for asymptotically small p, with an exponent dictated by local topology and force balance. We then develop an expression for the full distribution $P(p)$; though the treatment is approximate, it is sufficient to capture quantitatively the pressure statistics in the frictionless triangular lattice.

2.2.1. The statistics of small pressures. In the limit of small local pressure p, the local pressure distribution can be inferred directly from the distribution of global pressure $\mathcal{P}$. Note that equation (19) implies that the canonical distribution of $\mathcal{P}$ is proportional to $\Omega(\mathcal{P}) \exp(-\alpha\mathcal{P})$, which for small $\mathcal{P}$ scales as $\Omega(\mathcal{P})$. Recall that $\Omega(\mathcal{P}) \sim \mathcal{P}^{N_\mathrm{w}}$ and that N_w is the dimension of the space of networks with fixed $\mathcal{P}$. We can naively extrapolate this observation to the single-grain scale. A frictionless sphere with z_i contacts, and hence z_i contact forces, is subject to d force balance constraints. Therefore its configuration space at fixed pressure p_i has dimension $z_i - d - 1$. One therefore anticipates

$$P(p_i) \sim p_i^{z_i - d - 1}. \tag{25}$$

To test the reasonableness of this extrapolation, we perform numerical simulations of the FNE in a disordered packing. We sample the conditional probability distribution $P(p|z)$, i.e. the probability of obtaining a pressure p given that a grain has z contacts. Because the resulting curves are smoother, we plot the cumulative distribution $C_z(p) := \int_0^p \mathrm{d}p' P(p'|z)$. Figure 4 plots $\log C_z(p)$ versus $(z - d) \log p$ for a frictionless system; the linearity of the curves for small p confirms equation (25).

There is no *a priori* reason that it should be possible to extrapolate a local scaling from a macroscopic result. That such an extrapolation succeeds strongly suggests that

J. Stat. Mech. (2011) P04002

spatial correlations among the local pressures are weak; in section 2.4 we confirm that this is indeed the case. We stress the implication of equation (25): for weak interactions, the scaling of the pressure probability distribution can be inferred from simple degree of freedom counting codifying local topology and constraints, along with the flat measure on the ensemble.

The success of the above approach to asymptotically small pressures suggests that it is possible to adopt a 'single-grain picture', i.e. to simplify calculations by neglecting interactions with neighboring grains, and still successfully predict local pressure statistics. An approximate treatment of the statistics of local pressure in a single-grain picture can be surprisingly accurate, even for $p \gtrsim \langle p \rangle$ [8]. We now describe this approach. To do so we need a construct called the Maxwell–Cremona diagram, which we describe first.

2.3. Maxwell–Cremona diagrams

Contact forces in a packing may be used to construct a Maxwell–Cremona diagram [31], in which pairs of action–reaction forces between grains are mapped to a tiling of the plane. An edge in the tiling has a length proportional to the magnitude of the corresponding force, and its orientation is perpendicular to the vector force. This is most easily seen graphically (figures 5(a)–(c)): the boundary of a tile is constructed by rotating the vector forces acting on a grain by $\pi/2$ and placing them end to end in a right-hand fashion. Because the boundary is the vector sum of the contact forces acting on the grain, the boundary is closed (a polygon) whenever the grain is in force balance and not subject to body forces. Though the tiling can be generalized to incorporate body forces [24], they will not be considered here.

By Newton's third law, tiles of contacting grains have faces of like length and orientation. Hence tiles may be placed next to each other seamlessly, and the Maxwell–Cremona diagram is built up tile by tile in this fashion. For a packing in static force balance subject to imposed forces at the boundary, the corresponding Maxwell–Cremona diagram has a closed boundary and no internal gaps, as illustrated in figures 5(d) and (e). For a periodic packing, the tiling is also periodic. The reciprocal space coordinates of the diagram's vertices are, after rotation by $-\pi/2$, the void forces of Satake [32] and equivalently the loop forces of Ball and Blumenfeld [33].

The reciprocal tiling exists as a consequence of static force balance in the packing. The construction makes no assumptions regarding the presence or absence of tangential or tensile forces, and torque balance is not a necessary condition for its existence. Nevertheless, all the force networks that we study here are noncohesive and (trivially) torque balanced.

We have now shown that in hyperstatic frictionless disc packings it is possible to construct a set of contact force rearrangements $\langle \delta \mathbf{f}_k \rangle$ that transform one force balanced force network into another. In introducing the force rearrangements we emphasized that they leave the stress tensor invariant. This is reflected in the reciprocal tiling.

Consider the periodic force network in figure 6(a) and its reciprocal tiling in figure 6(b). The packing has orthogonal primitive vectors $\vec{L}_1 = L_1\hat{e}_1$ and $\vec{L}_2 = L_2\hat{e}_2$, and any surface normal to $\hat{e}_i$ experiences a net compressive force $\vec{F}_i = \hat{\bar{\sigma}}\vec{L}_i$. Without loss

J. Stat. Mech. (2011) P04002

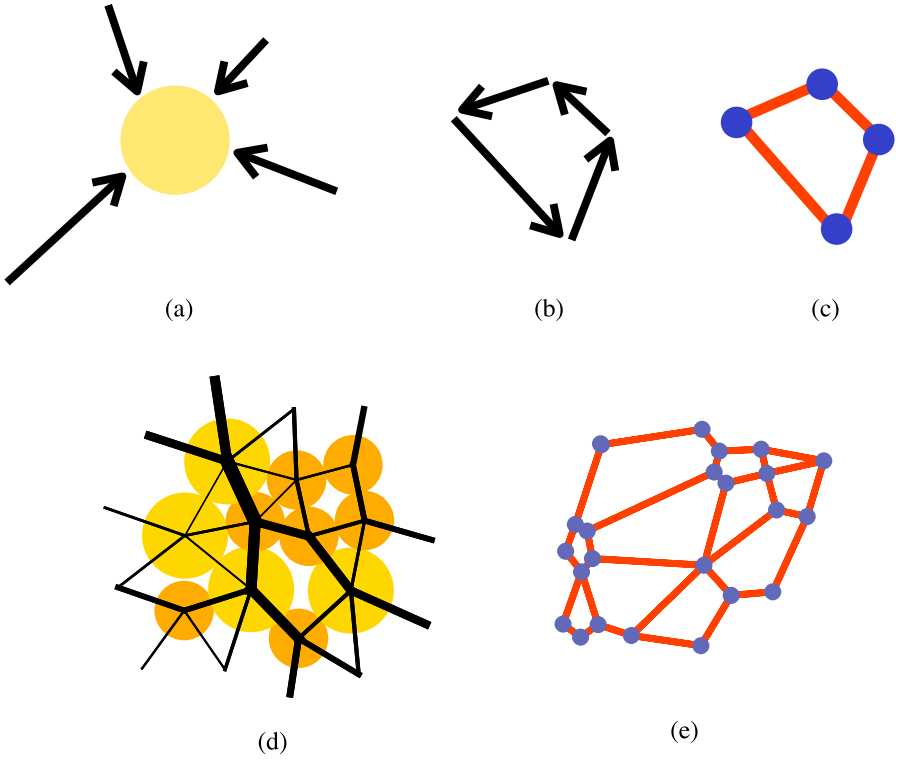

Figure 5. Constructing a tile in the Maxwell–Cremona diagram, or reciprocal tiling. (a) A disc with four contacts. Vector contact forces imposed by the neighboring discs are indicated by arrows. Note that the forces need not be frictionless, i.e. need not be parallel to the segment connecting the contacting discs' centers. (b) Each contact force is rotated by $\frac{\pi}{2}$ and drawn end to end, proceeding around the grain in a right-hand fashion. (c) The polygon enclosed by the vectors is the grain's corresponding tile in the tiling. The corners of the tile are vertices in the Maxwell–Cremona diagram. ((d), (e)) Due to Newton's third law, tiles corresponding to contacting grains can be placed flush against one another. The result is a tiling or tessellation. To determine the area of the tiling, it suffices to know the boundary forces on the packing; alternatively, one can sum the areas of individual tiles.

of generality we choose $\hat{e}_1$ and $\hat{e}_2$ to align with the principal stress directions, so that

$$\bar{\sigma}_{11} = \frac{F_1}{L_1}, \qquad \bar{\sigma}_{22} = \frac{F_2}{L_2}, \qquad \text{and} \qquad \bar{\sigma}_{12} = 0. \tag{26}$$

At the same time, by periodicity the tiling must have primitive vectors $\vec{F}_1$ and $\vec{F}_2$. Because the contact network is fixed in the FNE, the 'size and shape' of the tiling directly encodes the stress tensor via equations (26). In the following sections, the tiling's area $\mathcal{A}$ will play an important role. Note that

$$\mathcal{A} = F_1 F_2 = (\det \hat{\bar{\sigma}})\mathcal{V}, \tag{27}$$

J. Stat. Mech. (2011) P04002

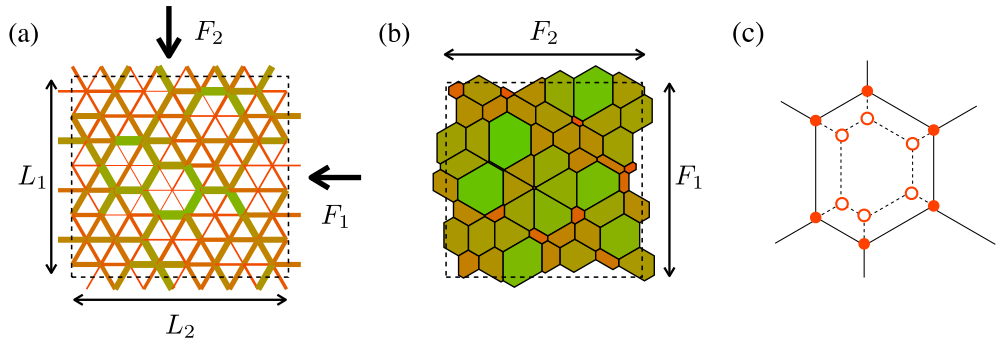

Figure 6. (a) A force network from the triangular lattice and (b) its Maxwell–Cremona diagram or reciprocal tiling. L_1 and L_2 are the dimensions of the unit cell. $\vec{F}_1$ and $\vec{F}_2$ are the forces transmitted across a plane normal to each of the primitive vectors. (c) Vertices in the tiling before (solid circles) and after (open circles) a force rearrangement.

and is therefore extensive. From the construction of the tiling, $\mathcal{A}$ is manifestly additive, $\mathcal{A} = \sum_{i=1}^{N} a_i$, where a_i, the area of the tile corresponding to grain i, is

$$a_i = \tfrac{1}{2}\hat{e}_3 \cdot \sum_{j=1}^{z_i} \vec{g}_j \times \vec{g}_{j+1}. \tag{28}$$

The sum runs over the z_i contacts of grain i in a right-hand sense, and indices are taken modulo z_i. The vector $\vec{g}_{j+1} := \sum_{k=1}^{j} \vec{f}_{jk}$. Note that $\vec{g}_1 = 0$. The unit vector $\hat{e}_3$ points out of the plane in a sense such that a_i is positive when all forces are compressive.

Equation (26) has important implications for the force network ensemble. To change the stress tensor or tiling area, a force rearrangement must change the primitive vectors of the reciprocal tiling's unit cell. A force rearrangement *cannot* change the primitive vectors $\vec{F}_1$ and $\vec{F}_2$: they were constructed with $\vec{F}_1$ and $\vec{F}_2$ fixed. As an example, consider the action of a wheel move in the triangular lattice, as in figure 6(c): the move simply shuffles area among the tiles, leaving the unit cell of the tiling unchanged. Therefore the stress tensor $\hat{\bar{\sigma}}$, or equivalently the extensive stress $\hat{\mathcal{S}} := \hat{\bar{\sigma}}\mathcal{V}$, is a topological invariant of the FNE, as is the tiling area $\mathcal{A}$, which is simply related to $\hat{\mathcal{S}}$ via equation (27). Nothing in this observation is particular to wheel moves, and so $\hat{\mathcal{S}}$ and $\mathcal{A}$ are invariant under force rearrangements in disordered force networks, as well.

2.3.1. The statistics of large pressures. We demonstrated above that a maximum entropy postulate correctly reproduces the appropriate equal *a priori* weighting of valid force networks in the microcanonical FNE, and used the same method to construct the canonical FNE. All of the results derived in this manner have direct analogs in equilibrium statistical mechanics. We now employ the principle of maximum entropy more broadly. When all that is known about a system is that it must satisfy certain constraints, the 'best guess' is that the system's state is described by a probability distribution that maximizes (information) entropy [36]. This statement reduces to the approach of section 2.1 if one imposes *all* the relevant constraints on the system, including the constraints of local force balance *on every grain*. Though these local constraints are

J. Stat. Mech. (2011) P04002

conceptually unproblematic and straightforward to implement in simulation, they render expressions like equations (24) difficult or impossible to evaluate. Because of these technical difficulties, we will seek to make approximations. In so doing, we take a simple lesson from information theory: the more information one incorporates (in the form of constraints on the system), the more accurate one can expect the predicted pressure distribution to be.

We now perform a calculation in which entropy is maximized subject to constraints on both $\langle \mathcal{P} \rangle$ and $\langle \mathcal{A} \rangle$ via Lagrange multipliers α and γ, respectively. We have seen that, in the presence of local force balance, these two constraints are redundant—see equation (27). However, we will also assume a single-grain picture in which interactions with neighboring grains are not explicitly incorporated. In so doing, the mechanism by which the constraints on $\langle \mathcal{P} \rangle$ and $\langle \mathcal{A} \rangle$ are redundant is broken: there is no tiling unless every grain is in local force balance. In this context, imposing the constraint on $\langle \mathcal{A} \rangle$, in addition to $\langle \mathcal{P} \rangle$, reintroduces some of the information that was lost by neglecting interactions. In effect, it tells the central grain something about the consequences of force balance on all the *other* grains in the system. The surprise is that with this one additional piece of information it is possible to describe local pressure distributions quantitatively. There is a price to be paid for this approach: because $\langle \mathcal{P} \rangle$ and $\langle \mathcal{A} \rangle$ are not independent constraints, the Lagrange multipliers α or γ introduced to impose them cannot be associated with true intensive thermodynamic parameters. Therefore α and γ within this approximate method should not be invested with any physical significance.

Here we will treat the case of the frictionless triangular lattice. The main simplification comes from the ordered contact network; we saw above that the pressure distribution $P(p)$ depends on the local coordination number. In a Bravais lattice, of course, each grain has the same number of contacts; in the triangular lattice, $P(p) \sim p^{z-d-1} = p^3$ for $p \to 0$. We have confirmed numerically that pressure statistics in disordered systems are similar to those for the triangular lattice [9]; in particular, their tails have the same qualitative form and, as shown above, they obey equation (25). However, the disordered case requires extending the theory to account for how pressure and tiling area are distributed among subpopulations with different local coordination numbers. This is an interesting question that we leave to future work.

In light of the above discussion, we identify the single-grain state with its pressure p and tiling area a and approximate the entropy of the system as $S = Ns$, where the single-grain entropy s is

$$s[b] = -\int_0^\infty \mathrm{d}p \int_0^\infty \mathrm{d}a\, v(p,a)\,[b(p,a)\ln b(p,a)]\,, \tag{29}$$

to be maximized subject to

$$\begin{aligned} 1 &= \int_0^\infty \mathrm{d}p \int_0^\infty \mathrm{d}a\, v(p,a) b(p,a) \qquad \langle p \rangle = \int_0^\infty \mathrm{d}p \int_0^\infty \mathrm{d}a\, v(p,a) p b(p,a) \\ \langle a \rangle &= \int_0^\infty \mathrm{d}p \int_0^\infty \mathrm{d}a\, v(p,a) a b(p,a). \end{aligned} \tag{30}$$

J. Stat. Mech. (2011) P04002

Here $\upsilon(p,a)$ is the single-grain density of states with pressure p and tiling area a. The result is $b(p,a) \propto \exp(-\alpha p - \gamma a)$, and the joint distribution $P(p,a)$ is

$$P(p,a) = Z^{-1}\upsilon(p,a)\exp(-\alpha p - \gamma a). \tag{31}$$

The Lagrange multipliers Z, α, and γ are determined via equations (30).

It is convenient to factorize $\upsilon(p,a) = \omega(p)\psi(a|p)$, where $\omega(p) = \int \mathrm{d}a\,\upsilon(p,a)$ is the single-grain density of states with pressure p. It is given by the right-hand side of equation (25), and therefore $\omega(p) \sim p^3$ in the frictionless triangular lattice. $\psi(a|p) = \upsilon(p,a)/\omega(p)$ is the density of single-grain states with tiling area a, given that the grain has a pressure p. We will assume for now, and confirm below, that $\psi(a|p)$ is peaked at a value $a^*(p) \approx \langle a(p)\rangle$; that is, given a pressure p, the most likely value of the tiling area (the mode of $\psi(a|p)$) is well approximated by the mean area of tiles with pressure p. Under this assumption,

$$\int_0^\infty \mathrm{d}a\,\psi(a|p)\exp(-\gamma a) \approx \exp(-\gamma\langle a(p)\rangle), \tag{32}$$

up to a prefactor that can be absorbed in Z. The local pressure probability distribution is $P(p) = \int_0^\infty \mathrm{d}a\,P(p,a)$, which becomes

$$P(p) = Z^{-1}p^3\exp(-\alpha p - \gamma\langle a(p)\rangle). \tag{33}$$

Thus the problem has been reduced to that of finding $\langle a(p)\rangle$.

Recall that in the reciprocal tiling, lengths are proportional to forces in the force network. In the triangular lattice, therefore, the pressure p on a grain is directly proportional to the perimeter of the corresponding tile. Therefore, in the simplest possible scenario, one anticipates from dimensional analysis $\langle a(p)\rangle \propto p^2$. In the frictionless triangular lattice, the area $a(p)$ of a tile with pressure (perimeter) p is bounded by the area of a regular hexagon with the same perimeter

$$a(p) \le \frac{\sqrt{3}}{24}p^2 = \frac{\langle a\rangle}{\langle p\rangle^2}p^2. \tag{34}$$

This is plotted in figure 7, which shows that the actual behavior of $\langle a(p)\rangle$ is indeed quadratic, to good approximation, and comes close to saturating the regular hexagon bound. From a fit to the numerically sampled $\langle a(p)\rangle$ we determine

$$\langle a(p)\rangle \approx 0.893\frac{\langle a\rangle}{\langle p\rangle^2}p^2. \tag{35}$$

The pressure distribution $P(p)$, determined using equation (35), is plotted in figure 8. The agreement with the numerically sampled distribution is excellent. Numerical distributions are computed using umbrella sampling, which allows us to determine the tail of $P(p)$ extremely accurately; see the appendix for a description of the method. The prediction of equation (33) captures the cubic growth at small p (figure 8(b)), the peak near $p \approx \langle p\rangle = 6$ (figure 8(c)), and the Gaussian tail. The latter feature is best seen in figure 8(d), which plots $\log P(p)/p^3$ versus p^2. The numerical distributions approach a line with slope -1. Finite size systems fall off faster than a Gaussian, but deviations from Gaussian decay decrease with increasing N. Note that, had the mean area of a tile $\langle a\rangle$ not been imposed, we would have recovered a distribution with $\gamma = 0$, i.e. an exponential

J. Stat. Mech. (2011) P04002

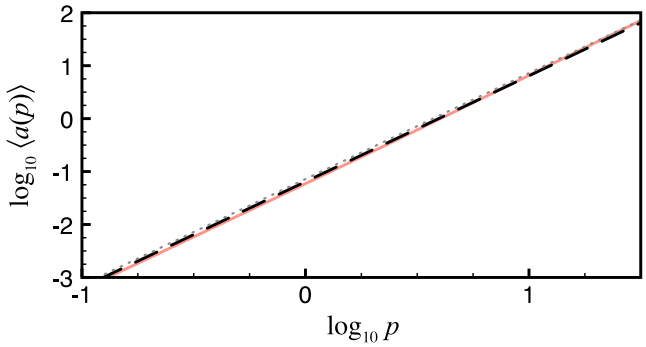

Figure 7. (solid curve) Numerically sampled average area $\langle a(p)\rangle$ of a tile in the triangular lattice, given that the corresponding grain has pressure p. Long dashed curve: fitted quadratic function $0.893(\langle a\rangle/\langle p\rangle)^2p^2$. Short dashed curve: area of a regular hexagon with perimeter p.

tail, in clear disagreement with the numerics. Thus the extra information provided by the tiling constraint has allowed us to capture the Gaussian tail of $P(p)$.

Recent years have seen considerable experimental, numerical, and theoretical work regarding the statistics of local stresses in static granular media. Notably, statistics in the FNE reproduce the main features of experimental measurements in packings of photoelastic discs [37]. It remains a subject of debate under what circumstances local stress distributions in granular media have Gaussian or exponential tails. This and other issues are summarized in a recent review by Tighe *et al* [9], to which we refer the interested reader.

2.4. Spatial correlations

A single-grain picture, which was employed above to describe $P(p)$ in the triangular lattice, cannot be expected to succeed in the presence of strong interactions, i.e. strong spatial correlations. We therefore seek now to characterize the correlations in the triangular lattice. Correlations may be conveniently characterized by the structure factors $\langle|p(\vec{q})|^2\rangle$ and $\langle|a(\vec{q})|^2\rangle$, where $\varphi(\vec{q}) = N^{-1}\sum_{\vec{r}}\varphi(\vec{r})e^{i\vec{q}\cdot\vec{r}}$ is the spatial Fourier transform of the position-dependent function $\varphi(\vec{r})$. A flat structure factor indicates the absence of spatial order. Figure 9 shows that the pressure and area structure factors for the triangular lattice are nearly flat, confirming that correlations are indeed weak.

The results of figure 9 may be partially motivated by considering the nontensile constraint. Each contact can sustain a normal force f which must be compressive; under our sign convention, this corresponds to a positivity constraint $f \geq 0$. A weaker constraint, which follows from positivity of the forces, is positivity of the pressure p on each grain. The converse is not true; pressure positivity does not guarantee force positivity. Nevertheless, arguments derived from pressure positivity are useful for developing intuition.

A stress state composed of the mean pressure $\langle p\rangle = p_0$ modulated by a single oscillatory mode $p_{\vec{r}} = p_0 + p_{\vec{q}}\cos(\vec{q}\cdot\vec{r})$ must obey $|p_{\vec{q}}| \leq p_0$. Noting that the resulting constraint on fluctuations is independent of q, we now assume that there is a typical scale $\tilde{p}$ for each $|p_{\vec{q}\neq 0}|$ and make a random phase approximation. Requiring $\langle(p_{\vec{q}} - p_0)^2\rangle \lesssim p_0^2$

J. Stat. Mech. (2011) P04002

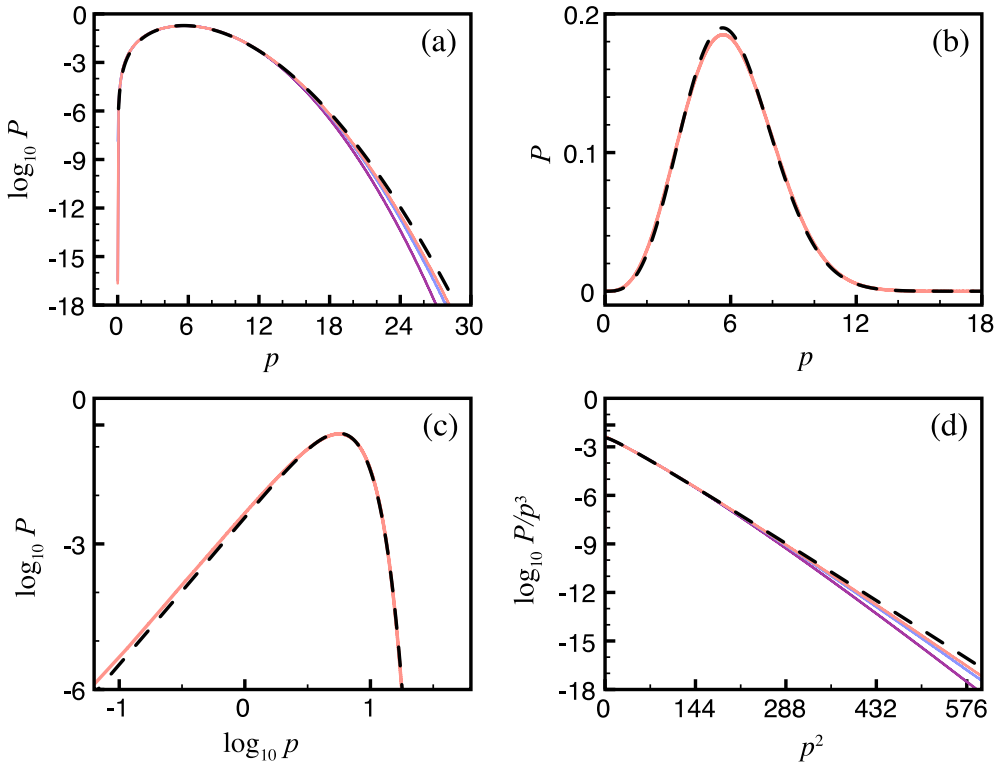

Figure 8. Numerics (solid curves) and equation (33) (dashed curves) for the local pressure probability distribution $P(p)$ in the frictionless triangular lattice of $N = 1840$ grains. The same data are shown in (a) semi-log, (b) linear–linear and (c) log–log plots, as well as (d) as $\log(P/p^3)$ versus p^2. To demonstrate finite size effects, (a) and (d) also contain data for $N = 460$ and 115.

then gives

$$\frac{\tilde{p}}{p_0} \lesssim \frac{1}{\sqrt{N}}. \tag{36}$$

A similar argument can be made for the area fluctuations. The ordinate axes in figure 9 have been rescaled to show that equation (36) holds.

Though spatial correlations are weak, they do have some influence on the local stress statistics. We now consider further the form of the area function $\langle a(p)\rangle$, which must be determined in order to predict $P(p)$ via equation (33). We argued above that $\langle a(p)\rangle \propto p^2$ is to be expected both on dimensional grounds and because $\langle a(p)\rangle$ is bounded by the area of the regular hexagon with perimeter p. We now show that, in a system truly devoid of interactions, one does indeed have purely quadratic scaling of $\langle a(p)\rangle$. We also show that there are in fact small corrections to quadratic scaling, which can therefore be attributed to spatial correlations.

Recalling that forces in a frictionless system are directed along contact normals, it is clear that the restriction to noncohesive forces also requires $a \geq 0$. For grain 1 with bond vectors $\{\vec{r}_{1j}\}$ there is also a maximum possible area $a_{\max}(p; \{\vec{r}_{1j}\})$. We have already noted that, in the triangular lattice, this maximum area corresponds to the regular hexagon with perimeter p. When interactions are neglected, each single-grain microstate has equal

J. Stat. Mech. (2011) P04002

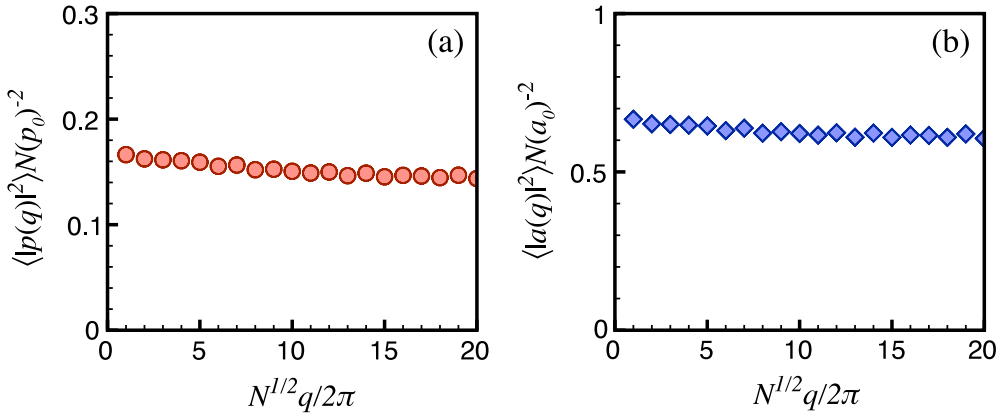

Figure 9. The structure factors (a) $\langle |p(\vec{q})|^2 \rangle$ and (b) $\langle |a(\vec{q})|^2 \rangle$ in the triangular lattice with $N = 1840$ grains. The wavevector $\vec{q}$ is parallel to a reciprocal lattice basis vector. The rescaling of the y-axis is suggested by equation (36). For uncorrelated variables the structure factor is flat.

a priori probability, independent of p and a. Moreover, whether the packing is ordered or disordered, scaling all the forces from a particular microstate of a grain by a scalar $\lambda > 0$ produces a new force balanced state such that $p \to \lambda p$ and $a \to \lambda^2 a$. Therefore, given the set of balanced states available for a particular $p > 0$, we may produce all the states for p' simply by scaling each microstate by $\lambda = p'/p$. The implication is that the conditional density of states $\psi(a|p)$ satisfies

$$\psi(a|p) = \lambda^2 \psi(\lambda^2 a|\lambda p). \tag{37}$$

Substituting this relation in $\langle a(p) \rangle = \int_0^\infty \mathrm{d}a\, a\psi(a|p)$, one finds $\langle a(p) \rangle = cp^2$ for some constant c. For packings under compressive stress, $\langle a \rangle > 0$, and therefore $c > 0$.

Because $\langle a(p) \rangle$ must be quadratic in systems without interactions, deviations from quadratic scaling are evidence of interactions. To show that there are (weak) interactions in the triangular lattice, we calculate the coefficient c directly assuming their absence. Namely,

$$\begin{aligned} \langle a(p) \rangle &= \eta^{-1} \int_0^\infty \mathrm{d}^6 f\, a(f_1 \ldots f_6) \times \delta\left(\sum_{i=1}^6 \vec{f}_i\right)\, \delta\left(\sum_{i=1}^6 f_i - p\right) \\ &= \frac{49}{60} \frac{\langle a \rangle}{\langle p \rangle^2} p^2 \end{aligned} \tag{38}$$

where $a(f_1, f_2, f_3, f_4, f_5, f_6)$ is the area of a tile given the grain's six forces and $\eta = \int \mathrm{d}^6 f\, \delta(\sum_{i=1}^6 \vec{f}_i)\delta(\sum_{i=1}^6 f_i - p)$. Replotting the data of figure 7 by dividing out a quadratic scaling in p, as in figure 10(a), reveals that $\langle a(p) \rangle$ in fact interpolates between two quadratic scalings. For asymptotically small p, the area function is given by equations (38), while for asymptotically large p it obeys equation (34) in equality. Therefore equation (35) should be interpreted as an effective scaling that compromises between these two quadratic scalings.

Similar behavior can also be seen in the conditional probability distribution $P(a|p)$. For smoother curves, figure 10(b) plots the integrated function $C_p(a) = \int_0^a \mathrm{d}a'\, P(a'|p)$.

J. Stat. Mech. (2011) P04002

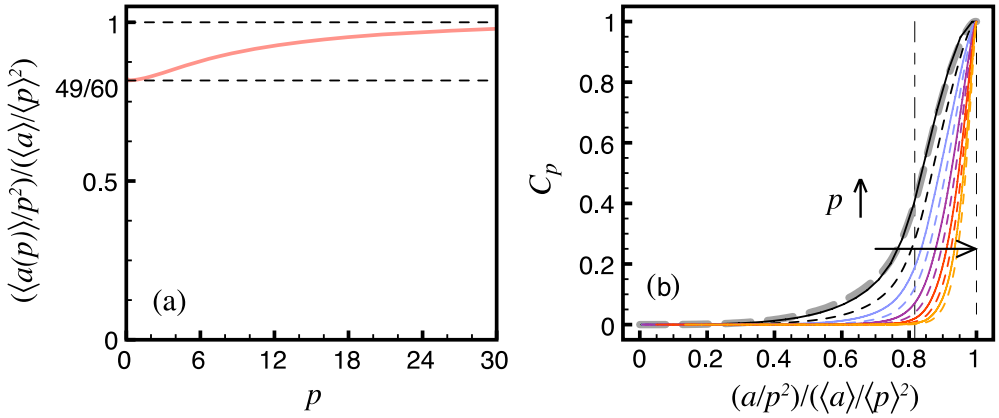

Figure 10. (a) Rescaled average area $p^{-2}\langle a(p)\rangle = p^{-2}\int_0^\infty \mathrm{d}a\, a\Psi(a|p)$ of a tile from a grain with pressure p. Dividing by p^2 makes it apparent that $\langle a(p)\rangle$ interpolates between two quadratic scalings. At small p the coefficient approaches that predicted by a calculation neglecting spatial correlations. For large p the coefficient approaches the upper bound given by a regular hexagon of perimeter p. (b) Statistics of tiles with an area a given that the tile has pressure ($\sim$ perimeter) p. For smoother curves the cumulative distribution $C_p(a) = \int_0^a \mathrm{d}a' P(a'|p)$ is plotted. Thin curves: cumulative distributions for $p = 2, 4, 6, \ldots, 20$, obtained using umbrella sampling. Thick dashed curve: $C_p(a)$ for a single-grain state in the absence of correlations with neighboring grains; the curve was determined by numerically sampling all *single-grain* force balanced states with a fixed pressure. Dashed vertical lines correspond to the asymptotes in (a).

If there were no spatial correlations in the system, plotting $C_p(a)$ against a/p^2 would collapse C_p to a master curve independent of p. This master curve is the single-grain density of states $\psi(a|p)$ in the absence of correlations, which can be obtained directly from Monte Carlo simulation of single-grain force balanced states. Deviations from the master curve indicate that there are some correlations in the system, consistent with the structure factors in figure 9. As expected from consideration of figure 10(a), for small p the cumulative distribution is in good agreement with the master curve. For asymptotically large p the function $C_p(a)$ approaches a step function near the upper bound corresponding to regular polygons, and $C_p(a)$ rises steeply over the whole range in p. This validates the approximation that $\int \mathrm{d}a\, \psi(a|p)\mathrm{e}^{-\gamma a} \approx \mathrm{e}^{-\gamma\langle a(p)\rangle}$, i.e. equation (32).

3. Discussion and outlook

We have demonstrated that ensembles of hyperstatic force networks subject to constraints of mechanical equilibrium can be described within a statistical mechanics framework. For a given contact geometry, the ensemble can be explored via force rearrangements that respect local force balance. The number of rearrangements is in proportion to the distance to isostaticity, Δz, and governs the macroscopic fluctuations of stress. In particular, pressure fluctuations in the FNE diverge in the isostatic limit and are characterized by a length scale $\ell_\mathrm{w} \sim \Delta z^{-1/d}$.

Local stress statistics can also be explored within the force network ensemble, and we have extracted considerable details regarding the distribution of grain scale pressures,

J. Stat. Mech. (2011) P04002

$P(p)$. In the limit of small pressures the distribution scales as a power law $P(p) \sim p^{z-d-1}$, with an exponent that reflects the local connectivity of the network and local force balance constraints. In the limit of large pressures the distribution displays a Gaussian tail in two dimensions; this may be understood as a consequence of the invariance of the reciprocal tiling area $\mathcal{A}$, which is quadratic in the forces.

The force network ensemble is a minimal model; it is useful to the degree that it captures features of static granular matter in simulations and experiments, but also insofar as it points out necessary ingredients of more realistic theories. In this sense it is complementary to recent experimental attempts to identify relevant state variables in static [38] and driven [39] athermal systems. One striking feature of the FNE is the Gaussian decay (in two dimensions) of the probability density of local pressures p or forces f. Early theoretical efforts such as the q-model predicted exponential tails but only incorporated *scalar* force balance [30]; we have seen that Gaussian tails are intimately connected to the reciprocal tiling, which requires vector force balance. The form of the tail of $P(f)$ in real granular systems is an interesting and open question; [9] summarizes recent theoretical, numerical, and experimental work on the matter.

The FNE is easily extended to frictional packings, and this is an obvious avenue of future research. The ensemble may also be used to study departures from equal *a priori* sampling of states, which are permitted in non-equilibrium ensembles.

Acknowledgments

We have benefited from helpful conversations with A R T van Eerd, M van Hecke, S Henkes, J H Snoeijer, J E S Socolar, and Z Zeravcic. BPT acknowledges support from the Netherlands Organization for Scientific Research (NWO).

Appendix. Umbrella sampling

In simulations we employ umbrella sampling, which permits extremely precise determination of the probability density of large stresses [7]. Monte Carlo simulations sample force networks $\mathbf{f}$ with a probability proportional to their statistical weight, i.e. in the force network ensemble each force network that satisfies local force balance and the boundary conditions is equally likely. As the vast majority of force networks only contain contact forces of order of magnitude $\langle f \rangle$, large contact forces or local pressures are hardly sampled and it is not possible to obtain $P(f)$ or $P(p)$ accurately for large f or p respectively.

To improve the sampling for large contact forces or local pressure, we employ the umbrella sampling method [40, 41]. The central idea is to create a bias in the force networks obtained in the Monte Carlo simulations, and to correct exactly for this bias afterward. To illustrate this, let us denote the *a priori* probability of a force network $\mathbf{f}$ by $G(\mathbf{f})$. In the force network ensemble $G(\mathbf{f})$ equals either 0 or 1. Monte Carlo simulations of the force network ensemble generate configurations with a probability proportional to $G(\mathbf{f})$, so therefore the average of a property A can be computed from

$$\langle A \rangle = \frac{\sum_{i=1}^{K} A(\mathbf{f}_i)}{K}, \tag{A.1}$$

J. Stat. Mech. (2011) P04002

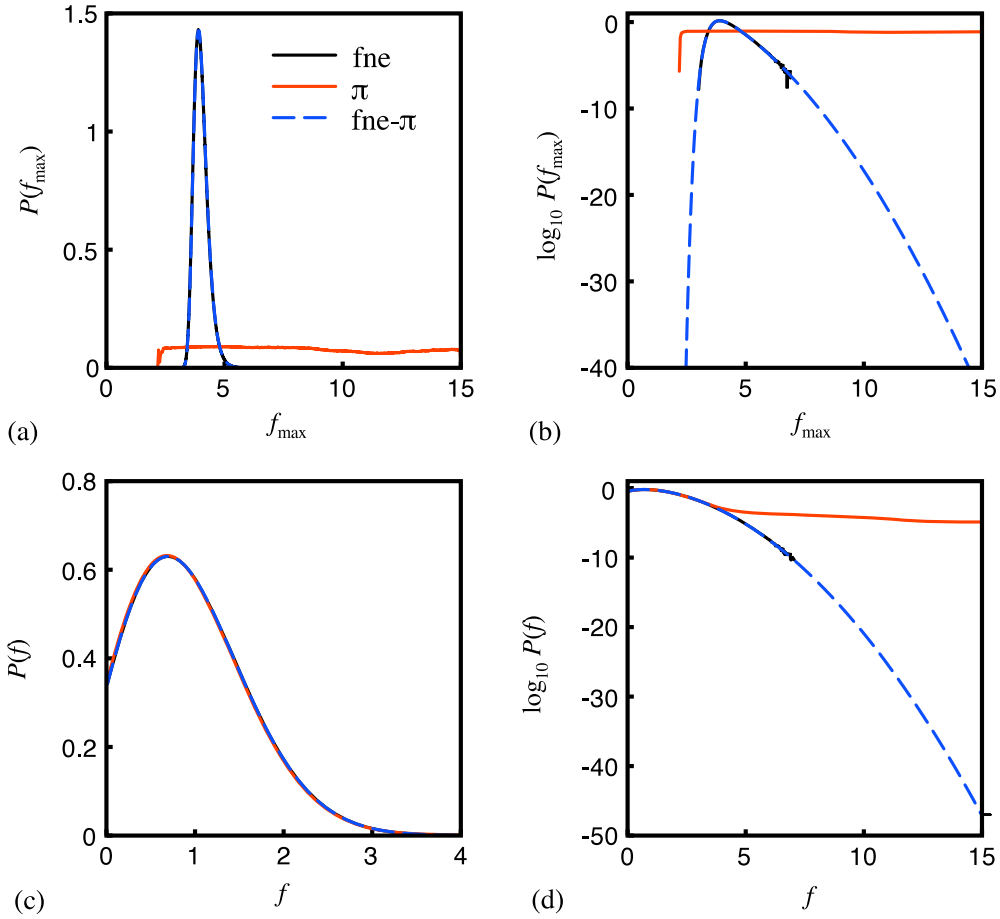

Figure A.1. ((a), (b)) Probability distributions of the maximum force $f_{\max}$ in a force network $\mathbf{f}$ and ((c), (d)) contact force distributions $P(f)$ for a frictionless triangular lattice ($N = 1840$). Three different situations are considered: (i) the force network ensemble without umbrella sampling (fne), (ii) the ensemble π in which $W(f_{\max})$ is chosen such that $P_\pi(f_{\max})$ is approximately flat (π), and (iii) the ensemble π in which ensemble averages are reweighted to the force network ensemble using equation (A.4) (fne-π). In all cases, the results for umbrella sampling (fne-π) are identical to those computed without umbrella sampling (fne). All forces are normalized such that $\langle f \rangle = 1$. Contact forces larger than $5\langle f \rangle$ are hardly sampled in the force network ensemble unless umbrella sampling is applied.

in which $\mathbf{f}_1, \mathbf{f}_2, \cdots, \mathbf{f}_K$ are the force networks generated by the Monte Carlo scheme. To generate more force networks with large forces, consider the ensemble π in which the *a priori* probability of a force network $\mathbf{f}$ equals

$$G_\pi(\mathbf{f}) = G(\mathbf{f}) \exp[W(\mathbf{f})], \tag{A.2}$$

in which $W(\mathbf{f})$ is an arbitrary function that only depends on the force network $\mathbf{f}$. Monte Carlo trial moves from state $\mathbf{f}_0$ to state $\mathbf{f}_n$ in this ensemble are thus accepted with a

J. Stat. Mech. (2011) P04002

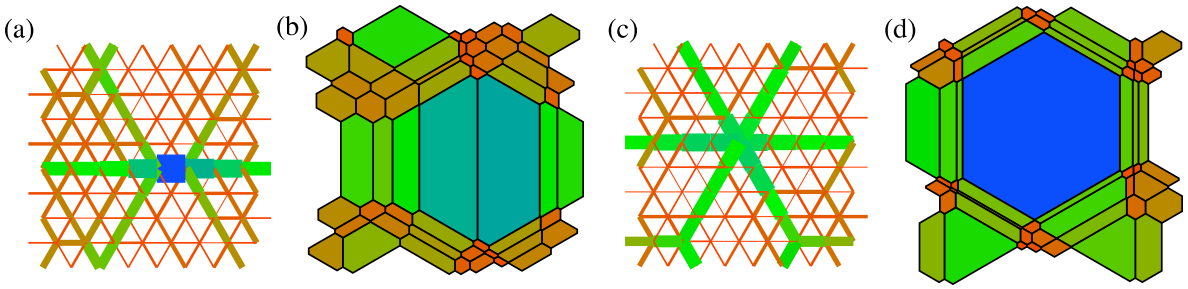

Figure A.2. (a) Typical force network containing a large contact force. Edge thicknesses are proportional to force magnitudes. (b) Reciprocal tiling of the force network in (a). (c) Typical force network containing a large local pressure (d) and its tiling. Colors map redundantly to force magnitudes or tile areas.

probability [42]

$$\mathrm{acc}(\mathbf{f}_0 \to \mathbf{f}_n) = \min\left(1, \frac{G(\mathbf{f}_n)}{G(\mathbf{f}_0)} \exp[W(\mathbf{f}_n) - W(\mathbf{f}_0)]\right). \tag{A.3}$$

Ensemble averages calculated in the ensemble π can easily be converted to ensemble averages in the original force network ensemble, as

$$\begin{aligned}\langle A \rangle &= \frac{\int \mathrm{d}\mathbf{f}\, G(\mathbf{f}) A(\mathbf{f})}{\int \mathrm{d}\mathbf{f}\, G(\mathbf{f})} \\ &= \frac{\int \mathrm{d}\mathbf{f}\, G(\mathbf{f}) \exp[W(\mathbf{f})] A(\mathbf{f}) \exp[-W(\mathbf{f})]}{\int \mathrm{d}\mathbf{f}\, G(\mathbf{f}) \exp[W(\mathbf{f})] \exp[-W(\mathbf{f})]} \\ &= \frac{\langle A(\mathbf{f}) \exp[-W(\mathbf{f})] \rangle_\pi}{\langle \exp[-W(\mathbf{f})] \rangle_\pi},\end{aligned} \tag{A.4}$$

in which we used the shorthand $\langle \cdots \rangle_\pi$ for averages computed in the ensemble π. A smart choice of $W(\mathbf{f})$ will sample many networks with large contact forces, so $P(f)$ can be computed accurately for large f. A convenient choice is to introduce the order parameter $f_{\max}(\mathbf{f})$ as the largest contact force of a force network $\mathbf{f}$ and to express W as a function of $f_{\max}$ only. The function $W(f_{\max}(\mathbf{f}))$ can be chosen such that the probability distribution $P_\pi(f_{\max})$ (computed in the modified ensemble) is approximately flat. As from equations (A.4) it follows that

$$P(f_{\max}) = \text{constant} \times P_\pi(f_{\max}) \exp[-W(f_{\max})], \tag{A.5}$$

it is convenient to iteratively determine $W(f_{\max})$ such that

$$W(f_{\max}) = -\ln P(f_{\max}). \tag{A.6}$$

To illustrate the use of umbrella simulations, in figure A.1 we have plotted the probability distributions of $P(f)$ and $P(f_{\max})$ computed with and without umbrella sampling for a frictionless triangular lattice of $N = 1840$ particles. From this figure it becomes clear that umbrella sampling increases the accuracy of $P(f)$ for large contact forces by many orders of magnitude.

To compute the probability distribution of local pressures $P(p)$ accurately for large p, we employ the same scheme. However, it turns out that configurations containing a

J. Stat. Mech. (2011) P04002

single large local pressure are qualitatively different from configurations containing a single large contact force. In the former, the large pressure is spread out over all contacts of the particle, while in the latter only two grains experience a large contact force. This is shown in figure A.2. As a consequence, to compute $P(p)$ accurately for large p a different order parameter is needed. In our simulations for computing $P(p)$, we choose $W = W(p_{\max}(\mathbf{f}))$ in which $p_{\max}(\mathbf{f})$ is the maximum local pressure of a force network $\mathbf{f}$.

References

[1] van Hecke M, *Jamming of soft particles: geometry, mechanics, scaling and isostaticity*, 2010 *J. Phys.: Condens. Matter* **22** 033101

[2] Snoeijer J H, Vlugt T J H, van Hecke M and van Saarloos W, *Force network ensemble: a new approach to static granular matter*, 2004 *Phys. Rev. Lett.* **92** 054302

[3] Tighe B P, Socolar J E S, Schaeffer D G, Mitchener W G and Huber M L, *Force distributions in a triangular lattice of rigid bars*, 2005 *Phys. Rev.* E **72** 031306

[4] Ostojic S and Panja D, *Elasticity from the force network ensemble in granular media*, 2006 *Phys. Rev. Lett.* **97** 208001

[5] Ostojic S, Somfai E and Nienhuis B, *Scale invariance and universality of force networks in static granular matter*, 2006 *Nature* **439** 828

[6] Snoeijer J H, Ellenbroek W G, Vlugt T J H and van Hecke M, *Sheared force networks: anisotropies and yielding and geometry*, 2006 *Phys. Rev. Lett.* **96** 098001

[7] van Eerd A R T, Ellenbroek W G, van Hecke M, Snoeijer J H and Vlugt T J H, *Tail of the contact force distribution in static granular materials*, 2007 *Phys. Rev.* E **75** 060302(R)

[8] Tighe B P, van Eerd A R T and Vlugt T J H, *Entropy maximization in the force network ensemble for granular solids*, 2008 *Phys. Rev. Lett.* **100** 238001

[9] Tighe B P, Snoeijer J H, Vlugt T J H and van Hecke M, *The force network ensemble for granular packings*, 2010 *Soft Matter* **6** 2908

[10] Alexander S, *Amorphous solids: their structure, lattice dynamics and elasticity*, 1998 *Phys. Rep.* **296** 65

[11] Moukarzel C, *Isostatic phase transition and instability in stiff granular materials*, 1998 *Phys. Rev. Lett.* **81** 1634

[12] Tkachenko A V and Witten T A, *Stress propagation through frictionless granular material*, 1999 *Phys. Rev.* E **60** 687

[13] Edwards S F and Oakeshott R B S, *Theory of powders*, 1989 *Physica* A **157** 1080

[14] Evesque P, *Boltzmann statistics of granular matter*, 1999 *Poudres Grains* **9** 13

[15] Kruyt N P and Rothenburg L, *Probability density functions of contact forces for cohesionless frictional granular materials*, 2002 *Int. J. Solids Struct.* **39** 571

[16] Bagi K, *Statistical analysis of contact force components in random granular assemblies*, 2003 *Granul. Matter* **5** 45

[17] Ngan A H W, *Mechanical analog of temperature for the description of force distribution in static granular packings*, 2003 *Phys. Rev.* E **68** 011301

[18] Goddard J D, *On entropy estimates of contact forces in static granular assemblies*, 2004 *Int. J. Solids Struct.* **41** 5851

[19] Henkes S, O'Hern C S and Chakraborty B, *Entropy and temperature of a static granular assembly: an ab initio approach*, 2007 *Phys. Rev. Lett.* **99** 038002

[20] Edwards S F, *The distribution of forces in a granular system under external stress is a spinglass problem*, 2008 *J. Phys.* A **41** 324019

[21] Philip T M, *H theorem for contact forces in granular materials*, 2008 *Phys. Rev.* E **77** 011307

[22] Henkes S and Chakraborty B, *Statistical mechanics framework for static granular matter*, 2009 *Phys. Rev.* E **79** 061301

[23] Snoeijer J H, Vlugt T J H, Ellenbroek W G, van Hecke M and van Leeuwen J M J, *Ensemble theory for force networks in hyperstatic granular matter*, 2004 *Phys. Rev.* E **70** 061306

[24] Tighe B P, *Granular lattice models with gravity*, 2009 *Powders and Grains 2009* ed M Nakagawa and S Luding (New York: American Institute of Physics) pp 305–8

[25] van Eerd A R T, Tighe B P and Vlugt T J H, *Numerical study of the force network ensemble*, 2009 *Mol. Simul.* **35** 1029

[26] McNamara S and Herrmann H, *Measurement of indeterminacy in packings of perfectly rigid disks*, 2004 *Phys. Rev.* E **70** 061303

J. Stat. Mech. (2011) P04002

[27] Unger T, Kertész J and Wolf D, *Force indeterminacy in the jammed state of hard disks*, 2005 *Phys. Rev. Lett.* **94** 178001
[28] Mailman M and Chakraborty B, *Unjamming of granular packings as a constraint satisfaction problem: evidence for a growing static length scale in frictionless packings*, 2010 arXiv:1007.0266v1
[29] Ostojic S, Vlugt T J H and Nienhuis B, *Universal anisotropy in force networks under shear*, 2007 *Phys. Rev.* E **75** 030301(R)
[30] Coppersmith S N, Liu C, Majumdar S, Narayan O and Witten T A, *Model for force fluctuations in bead packs*, 1996 *Phys. Rev.* E **53** 4673
[31] Maxwell J C, *Relaxing in foam*, 1864 *Phil. Mag.* **27** 250
[32] Satake R, *New formulation of graph theoretical approach in the mechanics of granular materials*, 1993 *Mech. Mater.* **16** 65
[33] Ball R C and Blumenfeld R, *Stress field in granular systems: loop forces and potential formulation*, 2002 *Phys. Rev. Lett.* **88** 115505
[34] Tighe B P and Vlugt T J H, *Force balance in canonical ensembles of static granular packings*, 2010 *J. Stat. Mech.* P01015
[35] Chandler D, 1987 *Introduction to Modern Statistical Mechanics* (New York: Oxford University Press)
[36] Jaynes E T, 1957 *Phys. Rev.* **106** 620
[37] Majmudar T S and Behringer R P, *Contact force measurements and stress-induced anisotropy in granular materials*, 2005 *Nature* **435** 1079
[38] Pugnaloni L A, Maza D, Sánchez I, Gago P A, Damas J and Zuriguel I, *Towards a relevant set of state variables to describe static granular packings*, 2010 *Phys. Rev.* E **82** 050301(R)
[39] Lechenault F and Daniels K E, *Equilibration of granular subsystems*, 2010 *Soft Matter* **6** 3074
[40] Torrie G M and Valleau J P, *Nonphysical sampling distributions in Monte Carlo free-energy estimation: umbrella sampling*, 1977 *J. Comput. Phys.* **23** 187
[41] Frenkel D and Smit B, 2002 *Understanding Molecular Simulation: from Algorithms to Applications* (San Diego, CA: Academic)
[42] Metropolis N, Rosenbluth A W, Rosenbluth M N, Teller A N and Teller E, *Nonphysical sampling distributions in Monte Carlo free-energy estimation: umbrella sampling*, 1953 *J. Chem. Phys.* **21** 1087

J. Stat. Mech. (2011) P04002